

Substantial Impact of Post Vaccination Contacts on Cumulative Infections during Viral Epidemics

Nash D. Rochman^{1,*}, Yuri I. Wolf¹, and Eugene V. Koonin^{1,*}

¹National Center for Biotechnology Information, National Library of Medicine, Bethesda, MD 20894

For correspondence: nash.rochman@nih.gov, koonin@ncbi.nlm.nih.gov

Keywords: SARS-CoV-2, Vaccine Escape, Vaccine Resistance, compartment model

12 **Abstract:**

13

14 **Background:** The start of 2021 will be marked by a global vaccination campaign
15 against the novel coronavirus SARS-CoV-2. Formulating an optimal distribution strategy
16 under social and economic constraints is challenging. Optimal distribution is additionally
17 constrained by the potential emergence of vaccine resistance. Analogous to chronic
18 low-dose antibiotic exposure, recently inoculated individuals who are not yet immune
19 play an outsized role in the emergence of resistance. Classical epidemiological
20 modelling is well suited to explore how the behavior of the inoculated population
21 impacts the total number of infections over the entirety of an epidemic.

22 **Methods:** A deterministic model of epidemic evolution is analyzed, with 7
23 compartments defined by their relationship to the emergence of vaccine-resistant
24 mutants and representing three susceptible populations, three infected populations, and
25 one recovered population. This minimally computationally intensive design enables
26 simulation of epidemics across a broad parameter space. The results are used to
27 identify conditions minimizing the cumulative number of infections.

28 **Results:** When an escape variant is only modestly less infectious than the originating
29 strain within a naïve population, there exists an optimal rate of vaccine distribution.
30 Exceeding this rate increases the cumulative number of infections due to vaccine
31 escape. Analysis of the model also demonstrates that inoculated individuals play a
32 major role in the mitigation or exacerbation of vaccine-resistant outbreaks. Modulating
33 the rate of host-host contact for the inoculated population by less than an order of
34 magnitude can alter the cumulative number of infections by more than 20%.

35 **Conclusions:** Mathematical modeling shows that optimization of the vaccination rate
36 and limiting post-vaccination contacts can affect the course of an epidemic. Given the
37 relatively short window between inoculation and the acquisition of immunity, these
38 results might merit consideration for an immediate, practical public health response.

39

40 **Introduction:**

41
42 The emergence of the novel Severe Acute Respiratory Syndrome Coronavirus 2
43 (SARS-CoV-2) responsible for the Covid-19 pandemic motivated dramatic public health
44 intervention including recommendations for isolation and quarantine throughout most of
45 2020¹. The beginning of 2021 will be marked by widespread vaccine distribution.
46 Optimizing distribution is challenging and subject to a myriad of social and economic
47 constraints²⁻⁴. The potential emergence of vaccine-resistant variants of the virus^{5,6}
48 introduces additional complications. Vaccination applies new selective pressures which
49 can lead to diverse intermediate outcomes even under conditions admitting eventual
50 pathogen eradication⁷⁻¹³. The larger the size of the vaccinated population, the greater
51 the pressure towards escape of vaccine-resistant variants.

52
53 Escape variants emerge within individual hosts after infection with the originating strain.
54 Naïve, unvaccinated, hosts are more easily infected than vaccinated hosts but
55 mutations conferring resistance are unlikely to provide a selective advantage in the
56 naïve background. Thus, naïve hosts are likely to shed escape variants at very low,
57 likely, negligible rates. The reverse is true for vaccinated hosts. Recently vaccinated,
58 inoculated, hosts that are not yet immune remain highly susceptible to infection with the
59 originating strain, and in these hosts, mutations conferring resistance are more likely to
60 provide a selective advantage. As a result, a substantial fraction or even most of the
61 virus shed by such hosts will be resistant mutants. This situation is analogous to the
62 administration of a low-dose antibiotic regime^{14,15}. In both cases, the pathogen is
63 introduced to a susceptible host and subject to elevated selective pressure towards the
64 emergence of resistant (escape) variants.

65
66 We sought to establish the constraints imposed by virus escape on optimal vaccine
67 distribution and the role played by the small, but critical, population of inoculated hosts.
68 To this end, we constructed an epidemiological compartment model to simulate
69 vaccination campaigns over a broad parameter regime. This minimally computationally

70 intensive approach enabled us to simulate many possible scenarios for epidemic
71 evolution, in order to determine the optimal vaccination strategy for each condition.

72

73 **Methods:**

74

75 We divided the population into 7 compartments (Fig. 1A). Three compartments are
76 susceptible to infection by either the originating strain or escape mutants: Naïve (N ,
77 unvaccinated and fully susceptible to the originating strain and escape mutants),
78 Inoculated (I , recently vaccinated and still partially susceptible to the originating strain,
79 and fully susceptible to escape mutants), and Vaccinated (V , minimally susceptible to
80 the originating strain, but fully susceptible to escape mutants). Two compartments
81 represent ongoing infection with the originating strain and are distinguished by the
82 host's previous compartment: Infected-Naïve (F) and Infected-Inoculated (M). The third
83 infected compartment represents infection by an escape variant, Infected-Escape (E).
84 The remaining compartment, Recovered (R), contains all hosts who were previously
85 infected. Vaccination is represented by a reduction in susceptibility to infection with the
86 originating strain. Naïve hosts are inoculated at rate k_v . Inoculated hosts do not
87 immediately acquire immunity and mature into the vaccinated compartment at rate k_m .
88 All infected hosts recover at rate k_r .

89

90 Within the timescale of the model, recovery is assumed to grant stable immunity, and
91 any variation in population size due to birth/death is assumed to be negligible. It should
92 be noted that, if recovery from the Infected-Naïve or Infected-Inoculated compartments
93 does not confer immunity against escape infection, the key results in this work will have
94 an even greater impact on the vaccination outcome. Hosts come into contact at rate k_c .
95 For simplicity, we assume that contact with an escape-infected host can only produce
96 an escape infection. Also, vaccine efficacy is assumed to be perfect such that
97 vaccinated hosts cannot be infected with the originating strain. The Inoculated-Infected
98 compartment is assumed to represent a symmetric composition of escape and
99 originating infections such that the total probability of a Naïve or Inoculated host being
100 infected after contact with a Naïve-Infected or Inoculated-Infected host is the same.

101 Finally, we assume that the probability of escape-infection is the same for Naïve and
102 Vaccinated hosts across all three types of infected-susceptible host interactions. This
103 construction yields the following transition probability matrices for Naïve, Inoculated,
104 and Vaccinated hosts:

$$105 \quad k_C P_N = k_I \begin{bmatrix} 1 & 0 & \alpha \\ 1 - \beta & 0 & \alpha + \beta \\ 0 & 0 & \beta \end{bmatrix}; k_C P_I = k_I \begin{bmatrix} 0 & 1 + \alpha & 0 \\ 0 & 1 + \alpha & 0 \\ 0 & 0 & \beta \end{bmatrix}; k_C P_V = k_I \begin{bmatrix} 0 & 0 & \alpha \\ 0 & 0 & \alpha + \beta \\ 0 & 0 & \beta \end{bmatrix}$$

106 where k_I represents the rate of infection for Naïve, Infected-Naïve host interactions
107 which is determined both by the contact rate k_C and the infectivity of the originating
108 strain. Rows represent interaction with each of the infected compartments (Infected-
109 Naïve, Infected-Inoculated, and Infected-Escape). Columns represent transitions to
110 each of the infected compartments.

111
112 An escape mutant can emerge within an Infected-Naïve or Infected-Inoculated host.
113 The parameter α represents the infectivity of the escape variant relative to the
114 originating strain when a Naïve host interacts with an Infected-Naïve host. The
115 parameter β represents the infectivity of an escape variant when a Naïve host interacts
116 with an Infected-Escape host relative to the infectivity of the originating strain when a
117 Naïve host interacts with an Infected-Naïve host. Informally, α reflects the ratio of
118 escape variant to originating strain shed by Infected-Naïve hosts, whereas β reflects the
119 fitness of an escape variant relative to the originating strain. Finally, we introduce the
120 parameter q to represent the impact of varying the rate of host-host contact for
121 Inoculated hosts relative to that for the other compartments. $q > 1$ represents increased
122 contact, and $q < 1$ corresponds to decreased contact. This completes the model
123 description and structures the differential equations:

$$N' = -(k_V + k_I ((1 + \alpha) (F + M) + \beta E)) N$$

$$I' = k_V N - (k_M + qk_I ((1 + \alpha) (F + M) + \beta E)) I$$

$$V' = k_M I - k_I (\alpha F + (\alpha + \beta) M + \beta E) V$$

$$F' = k_I (NF + (1 - \beta) NM) - k_R F$$

$$M' = qk_I (1 + \alpha) (F + M) I - k_R M$$

$$E' = k_I ((\alpha F + (\alpha + \beta) M + \beta E) (N + V) + q\beta EI) - k_R E$$

$$R' = k_R (F + M + E)$$

124

125 $k_R = k_M = 1/7$ are fixed across all simulations representing a time to recovery and time
126 between inoculation and the acquisition of immunity of one week. Reducing k_I would
127 prolong the epidemic and reducing k_M would increase the size of the Inoculated
128 compartment.

129

130 k_I is the principal determinant of epidemic magnitude and duration, with larger k_I leading
131 to a greater cumulative number of infections over a shorter period of time (Fig. 1B).
132 However, feedback between the size of the infected population and the rate of host-host
133 contact as well as spatial structure can decouple these variables. Throughout this work,
134 k_I is set to a benchmark value of 0.2 resulting in 50% of the population being infected
135 over a period of approximately 4 months.

136

137 The values of α and β impact the size of the Infected-Escape compartment. Even in the
138 absence of vaccination, large α/β results in the emergence of would-be resistant
139 variants (Fig 1C). In all analyses in this work, α is fixed at the benchmark value of 0.001
140 resulting in a modest number of would-be resistant infections for β close to 1 in the
141 absence of vaccination. Although a larger α would result in a greater total number of

142 escape infections, the fraction of those infections attributable to contact with inoculated
143 hosts would be smaller.

144
145 The solutions of the ODEs were obtained using the MATLAB ode45 method¹⁶.
146 Epidemics are simulated until the size of the Recovery compartment at arbitrarily long
147 times is approached. The principal quantity of interest is the cumulative number of
148 infections. When k_v is selected to minimize this value, minima are found through explicit
149 simulation over a range of rates. In the subsequent analysis, some values are
150 expressed relative to the cumulative number of infections in the absence of vaccination,
151 $R_{Null} \sim 50\%$.

152
153 **Results:**

154
155 In addition to the rate of vaccination, the outcome of a vaccination campaign depends
156 on how far the epidemic has progressed before vaccination begins, which can be
157 measured by the relative size of the Recovered compartment. The results also depend
158 on β , informally, the fitness of an escape variant relative to the originating strain. We
159 considered two values for β (0.01, low; 0.875, high) and varied both the start and rate of
160 vaccination. When β is low, that is, the escape mutant is much less fit than the
161 originating strain (Fig. 2A), vaccinating earlier and distributing the vaccine faster
162 decreases the cumulative number of infections. If distribution is sufficiently prompt, the
163 cumulative number of infections becomes negligible.

164
165 However, the outcome substantially differs for high β (Fig. 2B). Due to the vaccine
166 escape, at high rates of distribution, the cumulative number of infections remains large.
167 Furthermore, there is an optimal rate of distribution such that exceeding this rate
168 increases the cumulative number of infections. In this regime, the benefit of reducing the
169 size of the population susceptible to infection by the originating strain is outweighed by
170 the cost of increasing the selective pressure for the emergence of escape variants. In all
171 subsequent analysis, the vaccination rate is varied but vaccination is fixed to begin
172 when 1% of the population has recovered from infection.

173
174 Infections can be mitigated by reducing host-host contact. We sought to determine how
175 perturbing the contact rates for hosts in the Inoculated compartment relative to that of all
176 other compartments, q , affects the outcome. For β ranging between 0.75 and 1, we
177 considered three relative contact rates, $q=[0.2, 1, 5]$ (Fig. 2C). Increasing the rate of host-
178 host contact only within this compartment has a significant impact on the cumulative
179 number of infections. The optimal vaccination rate is also perturbed. Furthermore, if the
180 optimal vaccination rate it exceeded, reducing q below 1 slows the accumulation of
181 infections (Fig. 2D). The converse is true for increasing q , and the landscape is similar
182 when vaccination falls below the optimal rate (Fig. 2E).

183
184 Having demonstrated how q perturbs the optimal vaccination rate and how reducing q
185 below 1 can mitigate or delay the cumulative number of infections even if this rate is not
186 met or, conversely, is exceeded, we sought to establish the impact of q on the
187 cumulative number of infections across a wide range of β at the optimal vaccination rate
188 for each condition (Fig. 3A). The cumulative number of infections is sensitive to q across
189 the entire range of β . Varying q within an order of magnitude can substantially aid or
190 hinder the vaccination campaign, and when $q \gg 1$, the optimal rate of vaccination is 0.
191 Note that the maximum vaccination rate considered is $k_v=0.03$ representing the
192 inoculation of 3% of Naïve hosts per day. This rate is sufficiently high that the
193 cumulative number of infections at this rate (Fig. 3B) is similar or higher compared to
194 the hypothetical case where the entire Naïve population is immediately inoculated (Fig.
195 3C). Some of these effects are not specific to the inoculated compartment. Increasing
196 the rate of contact for any arbitrary subpopulation can increase the cumulative number
197 of infections. We define the effective k_I , k_{Ieff} , such that the cumulative number of
198 infections for $k_I=k_{Ieff}$ and $q=1$ is equal to the cumulative number of infections for $k_I=0.2$
199 (the benchmark) and arbitrary q . Increasing q within an order of magnitude is equivalent
200 to substantially increasing k_I for the entire population for the entirety of the epidemic
201 (Fig. 3D).

202

203 We additionally consider the cumulative infections added or subtracted relative to the
204 outcome corresponding to $q=1$ and scaled by the fraction of infections due to vaccine
205 escape (Fig. 3E). Varying q within an order of magnitude alters the cumulative number
206 of infections added or subtracted by more than 20% of the cumulative number of
207 infections in the absence of vaccination, R_{Null} , again demonstrating the critical role
208 played by inoculated hosts with respect to vaccine escape. The landscape is similar
209 when then rate of vaccination is fixed (Fig. 3F).

210

211 **Discussion:**

212

213 Epidemics can be mitigated through the reduction of host-host contact (quarantines and
214 other similar measures) and vaccination. A reduction in contact carries non-negligible
215 social and economic burdens so that, when vaccination becomes possible, the
216 continuation of such interventions might appear unnecessarily costly. Formulating an
217 optimal vaccination strategy to balance these pressures is challenging and is further
218 complicated by the possibility of vaccine escape. Escape variants emerging as a result
219 of vaccination are not expected to be more infectious than the originating strain,
220 otherwise, such variants would likely already be in circulation prior to vaccination.
221 However, newly emergent variants are not always much less infectious and can be
222 responsible for non-negligible disease incidence^{17,18}. Here, we demonstrated that, even
223 when escape variants are modestly less infectious, there exists an optimal vaccination
224 distribution rate such that exceeding this rate increases the cumulative number of
225 infections. This optimal rate depends on the infectivity of the escape variants. Such a
226 prediction is impractical at the time of writing, that is, in the very first days of the
227 vaccination campaign, and the cost of overestimation of the optimal vaccination rate is
228 far less than that of underestimation. However, to our knowledge, this phenomenon,
229 analogous to the evolution of antibiotic resistance, is not widely appreciated and, as
230 such, seems to warrant discussion.

231

232 Of more practical concern is the role of inoculated hosts in the emergence of escape
233 variants. Within low-dose antibiotic regimes^{14,15}, hosts are susceptible to infection with

234 the originating variant, and in such hosts, the pathogen is subjected to elevated
235 selective pressures towards the emergence of resistance. Similarly, within inoculated
236 hosts, the virus is subjected to gradually increasing selective pressures towards the
237 emergence of resistance while the intra-host population remains sufficiently large to
238 explore a substantial fraction of the mutation space. We demonstrated that moderately
239 increasing or decreasing the host-host contact rates for inoculated hosts only can
240 substantially aid or hinder the vaccination campaign. The time between vaccination and
241 the acquisition of immunity can be readily approximated from clinical endpoints^{19,20} and
242 is likely to be short enough that the societal costs of limiting post-vaccination contact
243 would be outweighed by these benefits.

244

245 **Limitations:**

246

247 In this study, we leveraged classical modelling techniques to elucidate the factors that
248 could substantially impact the outcome of any vaccination campaign. Although these
249 results are broadly applicable, they are not necessarily instrumental for predicting
250 quantitative outcomes for the current SARS-CoV-2 pandemic or any other particular
251 epidemic. Similarly, the model presented in this study is not designed to forecast long-
252 term outcome, a topic that has been thoroughly addressed for the case of SARS-Cov-2
253 and more generally^{7-13,21-23}.

254

255 The results presented here appear to be of immediate interest in relation to the
256 vaccination campaign against SARS-Cov-2 that is beginning at the time of this writing.
257 However, although diversification of the virus is apparent²⁴⁻²⁶ and the potential for
258 escape is being actively investigated^{5,6,27,28}, it cannot be ruled out that all escape
259 variants have a substantially reduced infectivity, represented by $\beta \ll 1$, in which case the
260 highest possible vaccination rate will be optimal and the benefits specific to post-
261 vaccination contact limitation could be negligible.

262

263 **Conclusions:**

264

265 Depending on the infectivity of escaping, vaccine-resistant mutants, the optimal
266 vaccination rate with respect to the cumulative number of infections can be lower than
267 the maximum rate. Contact rates for inoculated hosts can have a substantial impact on
268 the outcomes of vaccination campaigns. Even a brief and moderate limitation of
269 contacts in this well-defined population can potentially mitigate epidemics. These results
270 might merit consideration for an immediate, practical public health response.

271

272 **Author Contributions:**

273

274 NDR, YIW, and EVK conceived of the study; NDR constructed the model; NDR, YIW,
275 and EVK analyzed data; NDR and EVK wrote the manuscript that was edited and
276 approved by all authors.

277

278 **Acknowledgements:**

279

280 The authors thank Koonin group members for helpful discussions. NDR, YIW, and EVK
281 are supported by the Intramural Research Program of the National Institutes of Health
282 (National Library of Medicine).

283

284 **References:**

285

- 286 1. CDC. Public Health Guidance for Potential COVID-19 Exposure Associated with Travel. 2020.
- 287 2. Neumann-Böhme S, Varghese NE, Sabat I, et al. Once we have it, will we use it? A European survey on
- 288 willingness to be vaccinated against COVID-19. *The European Journal of Health Economics*: Springer; 2020.
- 289 3. Quinn SC, Kumar S, Freimuth VS, Kidwell K, Musa D. Public willingness to take a vaccine or drug under
- 290 Emergency Use Authorization during the 2009 H1N1 pandemic. *Biosecurity and Biodefense Strategy, Practice, and Science* 2009; **7**(3): 275-90.
- 291
- 292 4. Mills MC, Salisbury D. The challenges of distributing COVID-19 vaccinations. *EClinicalMedicine* 2020.
- 293 5. Li Q, Wu J, Nie J, et al. The impact of mutations in SARS-CoV-2 spike on viral infectivity and antigenicity.
- 294 *Cell* 2020; **182**(5): 1284-94. e9.
- 295 6. Kennedy DA, Read AF. Monitor for COVID-19 vaccine resistance evolution during clinical trials. *PLoS*
- 296 *Biology* 2020; **18**(11): e3001000.
- 297 7. Magpantay F, King A, Rohani P. Age-structure and transient dynamics in epidemiological systems. *Journal*
- 298 *of the Royal Society Interface* 2019; **16**(156): 20190151.
- 299 8. Restif O, Grenfell BT. Integrating life history and cross-immunity into the evolutionary dynamics of
- 300 pathogens. *Proceedings of the Royal Society B: Biological Sciences* 2006; **273**(1585): 409-16.
- 301 9. Rodrigues HS, Monteiro MTT, Torres DF. Vaccination models and optimal control strategies to dengue.
- 302 *Mathematical biosciences* 2014; **247**: 1-12.
- 303 10. Safan M, Kretzschmar M, Hadelier KP. Vaccination based control of infections in SIRS models with
- 304 reinfection: special reference to pertussis. *Journal of mathematical biology* 2013; **67**(5): 1083-110.
- 305 11. Scherer A, McLean A. Mathematical models of vaccination. *British Medical Bulletin* 2002; **62**(1): 187-99.
- 306 12. van Boven M, Mooi FR, Schellekens JF, de Melker HE, Kretzschmar M. Pathogen adaptation under
- 307 imperfect vaccination: implications for pertussis. *Proceedings of the Royal Society B: Biological Sciences* 2005;
- 308 **272**(1572): 1617-24.
- 309 13. Gandon S, Day T. The evolutionary epidemiology of vaccination. *Journal of the Royal Society Interface*
- 310 2007; **4**(16): 803-17.
- 311 14. Livermore DM. Minimising antibiotic resistance. *The Lancet infectious diseases* 2005; **5**(7): 450-9.
- 312 15. Roberts JA, Kruger P, Paterson DL, Lipman J. Antibiotic resistance—what’s dosing got to do with it? *Critical*
- 313 *care medicine* 2008; **36**(8): 2433-40.
- 314 16. Shampine LF, Reichelt MW. The matlab ode suite. *SIAM journal on scientific computing* 1997; **18**(1): 1-22.
- 315 17. Carman WF, Karayiannis P, Waters J, et al. Vaccine-induced escape mutant of hepatitis B virus. *The Lancet*
- 316 1990; **336**(8711): 325-9.
- 317 18. Brueggemann AB, Pai R, Crook DW, Beall B. Vaccine escape recombinants emerge after pneumococcal
- 318 vaccination in the United States. *PLoS Pathog* 2007; **3**(11): e168.
- 319 19. Polack FP, Thomas SJ, Kitchin N, et al. Safety and efficacy of the BNT162b2 mRNA covid-19 vaccine. *New*
- 320 *England Journal of Medicine* 2020.
- 321 20. Zhang Y, Zeng G, Pan H, et al. Safety, tolerability, and immunogenicity of an inactivated SARS-CoV-2
- 322 vaccine in healthy adults aged 18–59 years: a randomised, double-blind, placebo-controlled, phase 1/2 clinical
- 323 trial. *The Lancet Infectious Diseases* 2020.
- 324 21. Saad-Roy CM, Wagner CE, Baker RE, et al. Immune life history, vaccination, and the dynamics of SARS-
- 325 CoV-2 over the next 5 years. *Science* 2020; **370**(6518): 811-8.
- 326 22. Day T, Gandon S, Lion S, Otto SP. On the evolutionary epidemiology of SARS-CoV-2. *Current Biology* 2020.
- 327 23. Rochman ND, Wolf YI, Koonin EV. Evolution of Human Respiratory Virus Epidemics. *medRxiv* 2020:
- 328 2020.11.23.20237503.
- 329 24. Kumar S, Tao Q, Weaver S, et al. An evolutionary portrait of the progenitor SARS-CoV-2 and its dominant
- 330 offshoots in COVID-19 pandemic. *bioRxiv* 2020.
- 331 25. Rochman ND, Wolf YI, Faure G, Zhang F, Koonin EV. Ongoing Global and Regional Adaptive Evolution of
- 332 SARS-CoV-2. *bioRxiv* 2020.
- 333 26. van Dorp L, Acman M, Richard D, et al. Emergence of genomic diversity and recurrent mutations in SARS-
- 334 CoV-2. *Infection, Genetics, Evolution* 2020: 104351.

- 335 27. Garrett ME, Galloway J, Chu HY, et al. High resolution profiling of pathways of escape for SARS-CoV-2
336 spike-binding antibodies. *bioRxiv* 2020.
- 337 28. Starr TN, Greaney AJ, Hilton SK, et al. Deep mutational scanning of SARS-CoV-2 receptor binding domain
338 reveals constraints on folding and ACE2 binding. *Cell* 2020; **182**(5): 1295-310. e20.
- 339
- 340

341

342 **Figure legends**

343

344 **Figure 1. The Model. A.** Schematic of the 7 compartment model with three susceptible,
345 three infected, and one recovered compartments. **B.** Simulated epidemics for
346 $k_I=[0.15,0.175,0.2(\text{solid line}),0.225,0.25]$, $\alpha=0.001$, $\beta=0.01$ **C.** The ratio of cumulative
347 escape infections to all cumulative infections for an epidemic over a range of α .
348 $\beta=[0.5,0.67,0.83,1]$, darker color indicates higher value, $k_I=0.2$. The dotted line specifies
349 the benchmark value of $\alpha=0.001$.

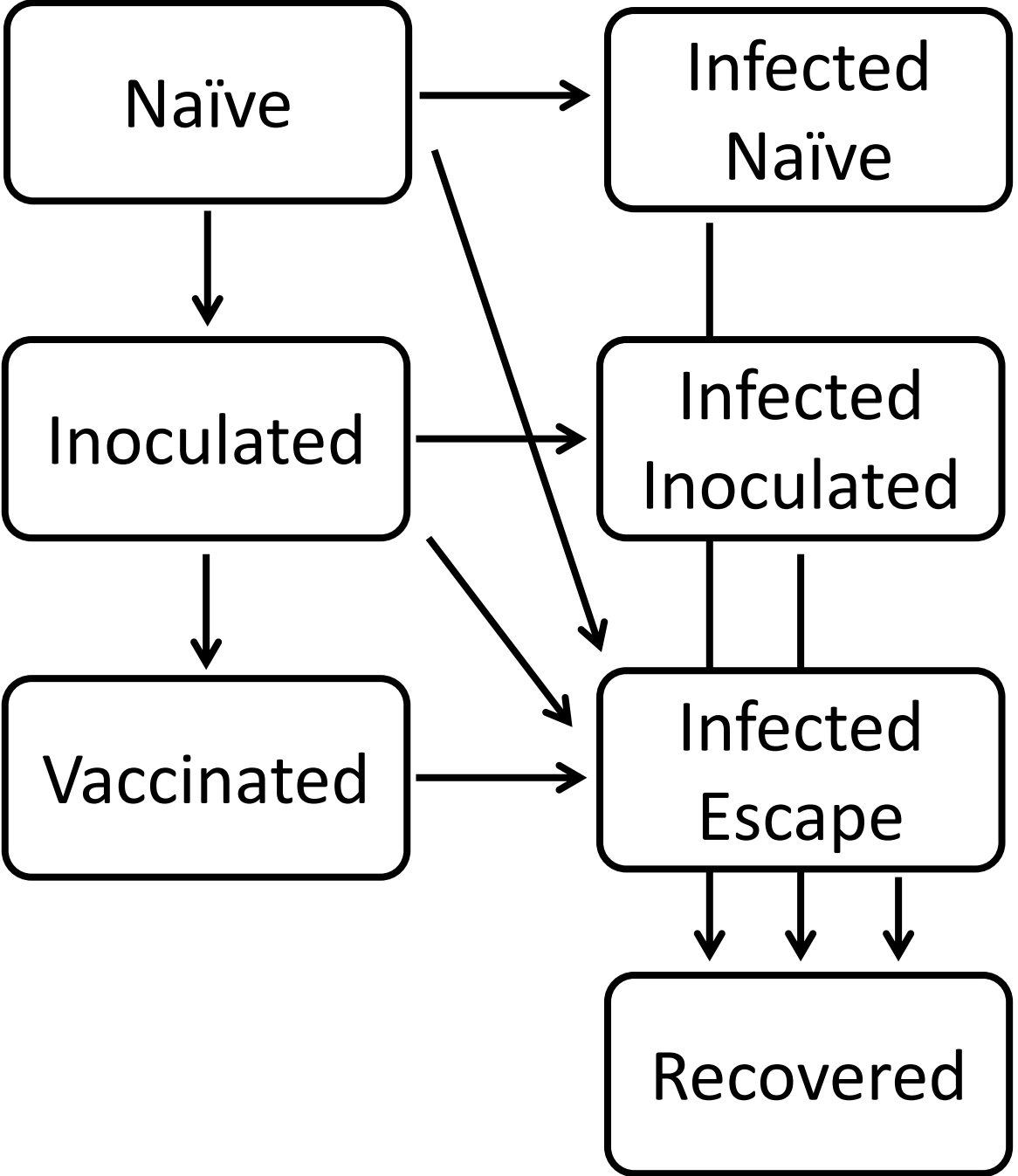
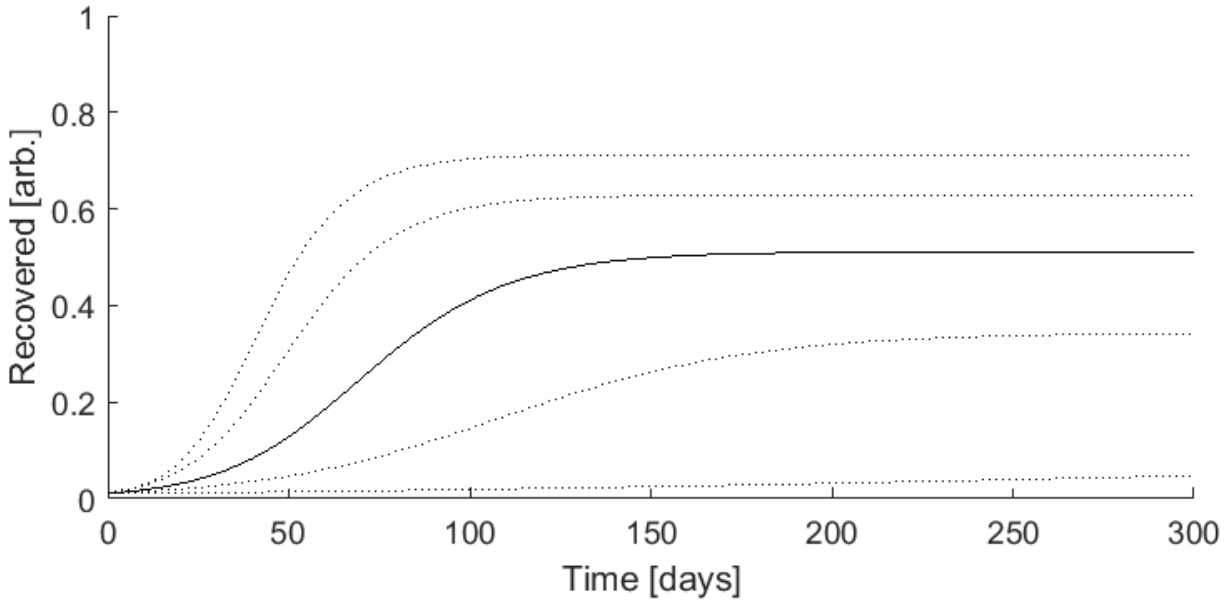
350

351 **Figure 2. Optimal Vaccine Distribution. A.** The cumulative number of infections
352 relative to no vaccination, R_{Null} , for a range of vaccine initiations and distribution rates.
353 Here β is low, 0.01. **B.** The cumulative number of infections relative to no vaccination,
354 R_{Null} , for a range of vaccine initiations and distribution rates and a large β (0.875). **A/B.**
355 3840 values were computed for each panel and 4x by 4x bilinearly interpolated points
356 are displayed. **C.** The cumulative number of infections relative to no vaccination, R_{Null} ,
357 for $\beta=[0.75(\text{dotted}),0.875(\text{dashed}),1(\text{solid})]$ and three relative contact rates,
358 $q=[0.2(\text{brown}),1(\text{black}),5(\text{gray})]$. **D.** Simulated epidemics comparing a high fixed rate of
359 vaccination, $k_V=0.03$ (solid) representing the inoculation of 3% of Naïve hosts per day,
360 and the optimal vaccination rate for each condition (dashed). $\beta=0.875$ is fixed and
361 $q=[0.2(\text{brown}),1(\text{black}),5(\text{gray})]$. **E.** Same as D. with a low fixed rate of vaccination,
362 $k_V=0.01$. **C/D/E.** The minima for the dashed lines in C correspond to the dashed lines in
363 D/E.

364

365 **Figure 3. Post-vaccination contacts. A.** The cumulative number of infections relative
366 to no vaccination, R_{Null} , for a range of β and q , optimizing k_V for each condition. **B.** Same
367 as in A. for fixed $k_V=0.03$ representing the inoculation of 3% of Naïve hosts per day. **C.**
368 Same as in A. for the case where all Naïve hosts are immediately inoculated. **D.** Log of
369 the effective k_I , k_I^{eff} , relative to $k_I=0.2$, the benchmark, vs. log of q for $\beta=[0.5$ (dotted
370 line), 0.7 (dashed line), 1 (solid line)]. **E.** The cumulative number of infections relative to
371 R_{Null} and $q=1$ scaled by the fraction of infections due to vaccine escape,

372 $\sum \text{Escape}(q) / \sum \text{Infections}(q) (\sum \text{Infections}(q) - \sum \text{Infections}(q=1)) / R_{\text{Null}}$, for a range of β and q ,
373 optimizing k_v for each condition. **F.** Same as in E for fixed $k_v=0.03$. **A-C/E/F.** 961 values
374 were computed for each panel and 4x by 4x bilinearly interpolated points are displayed.
375

A**B****C**